J. Fluid Mech. (1995), *vol.* 284, *pp.* 359–375

Trapping of water waves by submerged plates using hypersingular integral equations

By NEIL F. PARSONS AND P. A. MARTIN
Department of Mathematics, University of Manchester, Manchester M13 9PL, UK

(Received 23 June 1994)

The trapping of surface water waves by a thin plate in deep water is reduced to finding non-trivial solutions of a homogeneous, hypersingular integral equation for the discontinuity in velocity potential across the plate. The integral equation is discretized using an expansion-collocation method, involving Chebyshev polynomials of the second kind. A non-trivial solution to the problem is given by the vanishing of the determinant inherent in such a method. Results are given for inclined flat plates, and for curved plates that are symmetric with respect to a line drawn vertically through their centre. Comparisons with published results for horizontal flat plates (in water of finite depth) and for circular cylinders are made.

1. Introduction

Consider a three-dimensional ocean with cylindrical boundaries; examples are oceans of constant depth with long canyons or ridges, a long circular cylinder submerged parallel to the free surface, and a plane beach. Introduce Cartesian coordinates $Oxyz$, with the origin at a point in the mean free surface, the y-axis pointing vertically down into the water and the z-axis parallel to the generator of the boundaries, so that the x-axis is horizontal. We are interested in wave motions that are spatially periodic in the z-direction. A natural problem is the scattering by a horizontal circular cylinder of a regular surface wave at oblique incidence to the axis of the cylinder; the wave is partially reflected and partially transmitted, so that the scattered waves propagate to $x = \pm\infty$. However, we are interested here in modes of motion of a different kind, called *trapped modes*; these are free oscillations (no incident wave) characterized by exponential decay as $|x| \to \infty$.

It is known that some cylindrical structures can support trapped modes. In an oceanographical context, the basic geometry is a semi-infinite ocean, $x > 0$, with a shoreline at $x = 0$ and parallel depth contours, so that the sea floor is given by $y = h(x)$ for some function h. Much is known about the existence and consequences of trapped modes for such geometries, going back to the Stokes edge wave of 1846; see, for example, Ursell (1952), Meyer (1971), LeBlond & Mysak (1978, §25) and Bonnet-Ben Dhia & Joly (1993).

We shall be concerned with geometries of a different kind, where there is an infinite ocean of uniform depth (finite or infinite) containing a submerged horizontal cylinder with a bounded cross-section, Ω. The simplest configuration is a circular cylinder in deep water, so that Ω is a circle; assume that the centre of the circle is on the y-axis. Ursell (1951) proved that this configuration can support a trapped mode, which is an even function of x – a *symmetric mode*. His proof relies on the fact that the radius of

the cylinder is sufficiently small compared to the wavelength. However, this restriction is not a physical one, as was shown by Jones (1953); indeed, his argument proves the existence of symmetric modes for a wide class of symmetric cross-sections. McIver & Evans (1985) used Ursell's formulation as the basis for a numerical method, and found several modes above circular cylinders. Martin (1989) developed another numerical method, based on a boundary integral equation, and found good agreement with the results of McIver & Evans (1985). He also found numerical evidence to support the existence of *antisymmetric modes* (odd functions of x) above a circular cylinder, and various modes above elliptical cylinders, even when the cross-section is not symmetric about the y-axis.

In the present paper, we consider cylinders that have degenerated into thin rigid plates, motivated by a paper of Linton & Evans (1991). They considered a submerged, horizontal, flat plate in water of finite depth, and used a numerical method based on matched eigenfunction expansions. They found strong numerical evidence for the existence of trapped modes above such a plate. Here, we assume that the water is deep (this assumption could be relaxed), but we allow the plate to have different orientations (thus breaking the symmetry); we also consider *curved* plates. The method used is similar to that used by Parsons & Martin (1992, 1994) for analogous two-dimensional scattering problems: we reduce the problem to a hypersingular boundary integral equation for the discontinuity in the velocity potential across the plate. For trapped-mode problems, the integral equation is homogeneous, and so we expect non-trivial solutions only at discrete frequencies.

As in previous work, we approximate the solution of the integral equation by means of a truncated series of Chebyshev polynomials of the second kind, multiplied by a suitable weight function. Collocation then gives a homogeneous matrix equation for the unknown coefficients. A non-trivial solution is then implied by the vanishing of the determinant.

After formulating the problem for arbitrary plates, the paper has two sections, one on flat plates (§3) and one on curved plates (§4). We confirm the results of Linton & Evans (1991) for horizontal flat plates; symmetric and antisymmetric modes are found. Then, we follow these modes as the geometry is altered, either by rotating the plate or deforming the plate into the arc of a circle. In particular, as the arc approaches a complete circle, we find agreement with the corresponding modes computed by McIver & Evans (1985) for a circular cylinder. This agreement at both limits of the deformation (horizontal flat plate and solid circular cylinder), using three different numerical methods, suggests that the presented numerical results are correct, and that the method will be useful for other configurations.

2. Formulation

Consider a long thin plate, with cross-section Γ, submerged beneath the free surface of deep water. We look for standing-wave solutions of the corresponding three-dimensional boundary-value problem in the form

$$\Phi(x, y, z, t) = \phi(x, y) \cos lz \cos \omega t,$$

where l is the wavenumber in the z-direction, ω is the frequency and ϕ is a real potential. By combining solutions of this type (with other trigonometric variations in z and t), we can construct solutions for propagating waves. For example, it is known that the problem with $l < K$, where $K = \omega^2/g$ and g is the acceleration due to gravity, arises in the scattering of regular surface waves at oblique incidence

to the plate. However, for $l > K$, there may be discrete values of l for which a non-trivial ϕ exists, in the absence of any forcing or incident waves, and for which $\phi \to 0$, exponentially, as $x \to \infty$ (Ursell 1968 showed that if $|\text{grad}\,\phi| \to 0$ as $|x| \to \infty$, then ϕ necessarily decays exponentially). These are trapped modes. One can think of (suitable combinations of) them as waves that are guided by the plate.

The three-dimensional potential Φ satisfies Laplace's equation and the usual homogeneous boundary conditions. Thus, the two-dimensional potential $\phi(x, y)$ must satisfy the modified Helmholtz equation

$$\frac{\partial^2\phi}{\partial x^2} + \frac{\partial^2\phi}{\partial y^2} - l^2\phi = 0 \qquad \text{in the fluid,} \tag{2.1}$$

$$\phi l \cos\beta + \frac{\partial\phi}{\partial y} = 0 \qquad \text{on the free surface, } y = 0, \tag{2.2}$$

and

$$\frac{\partial\phi}{\partial n} = 0 \qquad \text{on the plate, } \Gamma; \tag{2.3}$$

$\partial/\partial n$ is normal differentiation on Γ. For trapped modes, we also require that

$$|\text{grad}\,\phi| \to 0 \qquad \text{as } x^2 + y^2 \to \infty. \tag{2.4}$$

Here, because of the assumption that $l > K$, we find it convenient to introduce a new variable β, defined by $K = l\cos\beta$. We call $l = K$ the *lower cut-off*.

An appropriate fundamental solution for this problem is given by (Ursell 1951)

$$G(P, Q) = K_0(lR) + K_0(lR_1) + 2\cot\beta\,\mathscr{G}(P, Q),$$

where $P \equiv (x, y)$ and $Q \equiv (\xi, \eta)$ are points in the fluid, K_n is the modified Bessel function of the second kind and order n,

$$\mathscr{G} = \int_0^\infty \frac{\sin\beta}{\cosh\mu - \cos\beta}\, e^{-lY\cosh\mu} \cos(lX\sinh\mu)\,d\mu, \tag{2.5}$$

$X = x - \xi$, $Y = y + \eta$, $R^2 = X^2 + (y - \eta)^2$ and $R_1^2 = X^2 + Y^2$. G satisfies (2.1), (2.2) and (2.4), and has a logarithmic singularity at $P = Q$.

$\mathscr{G}$ can be evaluated directly from (2.5) or from an expansion due to Ursell (1962),

$$\mathscr{G} = \sum_{m=0}^{\infty} \epsilon_m(-1)^m I_m(lR_1)\{(\pi - \beta)\cos m\Theta_1 \cos m\beta + \Theta_1 \sin m\Theta_1 \sin m\beta\}$$
$$- 2\sum_{m=1}^{\infty}(-1)^m L_m(lR_1)\cos m\Theta_1 \sin m\beta, \tag{2.6}$$

where $\epsilon_0 = 1$, $\epsilon_m = 2$ for $m > 0$ and $\Theta_1 = \tan^{-1}(X/Y)$. The function L_m is defined by

$$L_m(w) = \left[\frac{\partial}{\partial\nu} I_\nu(w)\right]_{\nu=m} \tag{2.7}$$

where I_ν is the modified Bessel function of the first kind; the computation of L_m is discussed in Appendix A.

We now apply Green's theorem to ϕ and G to give an integral representation for ϕ valid throughout the fluid domain. Thus, we find

$$2\pi\phi(P) = \int_\Gamma [\phi(q)]\frac{\partial G(P, q)}{\partial n_q} ds_q, \tag{2.8}$$

where $[\phi(q)]$ is the discontinuity in ϕ across the plate at q; we use the lower case letters p and q to denote points on the plate. Now, because G is logarithmically singular, it is known that when applying (2.3) to (2.8), it is permissible to interchange integration and normal differentiation, provided that the integration is redefined as a Hadamard finite-part integral; the legitimacy of this procedure has been proved by Martin & Rizzo (1989). Thus, we are led to consider the homogeneous, hypersingular integral equation

$$\text{⨍}\!\!\!\!\!\!-_{\Gamma} [\phi(q)] \frac{\partial^2 G(p,q)}{\partial n_p \partial n_q} \, \mathrm{d}s_q = 0, \qquad \text{for } p \in \Gamma, \tag{2.9}$$

which is to be solved subject to $[\phi] = 0$ at the two edges of Γ. (The cross on the integral sign in (2.9) signifies that it is to be interpreted in the finite-part sense; see Martin & Rizzo 1989 for definitions and further information.) Our aim is to find pairs of parameters l and β, with fixed geometries, for which non-trivial solutions to (2.9) exist.

2.1. *The kernel*

A general form of the kernel of (2.9) can be constructed for use with any Γ. Denote the unit normals at p and q by $\boldsymbol{n}(p) = (n_1^p, n_2^p)$ and $\boldsymbol{n}(q) = (n_1^q, n_2^q)$, respectively. Then, applying the formula

$$\frac{\partial^2 G}{\partial n_p \partial n_q} = n_1^p n_1^q \frac{\partial^2 G}{\partial x \partial \xi} + n_1^p n_2^q \frac{\partial^2 G}{\partial x \partial \eta} + n_2^p n_1^q \frac{\partial^2 G}{\partial y \partial \xi} + n_2^p n_2^q \frac{\partial^2 G}{\partial y \partial \eta}$$

to G, using the expansion (2.6), it can be shown (Parsons 1994) that the kernel takes the form

$$\frac{\partial^2 G(p,q)}{\partial n_p \partial n_q} = \frac{\mathscr{N}}{R^2} \{(lR) K_1(lR)\} - \frac{2\Theta}{R^4} \left\{ \frac{1}{2} (lR)^2 K_2(lR) \right\} + l^2 \mathscr{H}(X, Y), \tag{2.10}$$

where

$$\mathscr{N} = \boldsymbol{n}(p) \cdot \boldsymbol{n}(q), \; \Theta = (\boldsymbol{n}(p) \cdot \boldsymbol{R})(\boldsymbol{n}(q) \cdot \boldsymbol{R}), \; \boldsymbol{R} = (x - \xi, y - \eta), \; R = |\boldsymbol{R}|,$$

$$\mathscr{H}(X, Y) = \mathscr{N} \mathscr{H}_1 + \left(n_1^p n_2^q - n_2^p n_1^q\right) \mathscr{H}_2 + (n_1^p n_1^q - n_2^p n_2^q) \mathscr{H}_3, \tag{2.11}$$

$$\begin{aligned}
\mathscr{H}_1 &= \tfrac{1}{2} K_2(lR_1) \cos 2\Theta_1 + 2K_1(lR_1) \cos\Theta_1 \cos\beta + 2K_0(lR_1) \cos^2\beta - \mathscr{K}_1 \cot\beta \cos 2\beta, \\
\mathscr{H}_2 &= \tfrac{1}{2} K_2(lR_1) \sin 2\Theta_1 + 2K_1(lR_1) \sin\Theta_1 \cos\beta + 2\mathscr{K}_2 \cos^2\beta, \\
\mathscr{H}_3 &= -\tfrac{1}{2} K_0(lR_1) + \mathscr{K}_1 \cot\beta, \\
\mathscr{K}_1 &= 2 \sum_{m=1}^{\infty} (-1)^m L_m(lR_1) \cos m\Theta_1 \sin m\beta \\
&\qquad - \mathrm{e}^{-KY} \left[(\pi - \beta) \cosh(lX \sin\beta) - \Theta_1 \sinh(lX \sin\beta) \right], \\
\mathscr{K}_2 &= 2 \sum_{m=1}^{\infty} (-1)^m L_m(lR_1) \sin m\Theta_1 \cos m\beta \\
&\qquad - \mathrm{e}^{-KY} \left[(\pi - \beta) \sinh(lX \sin\beta) - \Theta_1 \cosh(lX \sin\beta) \right].
\end{aligned} \tag{2.12}$$

In (2.10), the terms in braces tend to one as $l \to 0$.

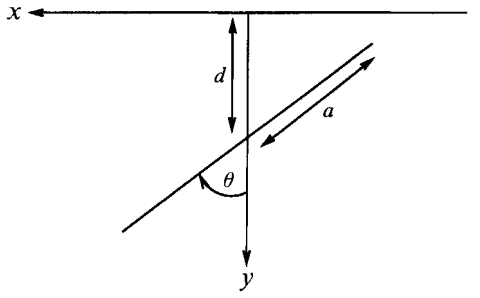

FIGURE 1. Geometry of the submerged, flat plate.

3. Flat plates

In this section, we consider the simplest case of a flat plate of length $2a$, inclined at an arbitrary angle θ to the vertical (figure 1).

3.1. *Method of solution*

We first parametrize the geometry in terms of a single parameter, thereby reducing the problem to a one-dimensional, hypersingular integral equation. A suitable parametrization of the plate is

$$\xi(t) = at\sin\theta, \qquad \eta(t) = d + at\cos\theta, \qquad -1 \leqslant t \leqslant 1,$$

where $q \equiv (\xi,\eta)$ and $|\theta| \leqslant \pi/2$; d is the submergence of the mid-point of the plate, and satisfies $d > a\cos\theta$ to ensure that the plate is completely submerged. The point $p \equiv (x,y)$ on Γ has the same parametrization, but with t replaced by s. It follows that $R = a|s-t|$, $\boldsymbol{n}(p) = \boldsymbol{n}(q) = (-\cos\theta, \sin\theta)$, $\mathcal{N} = 1$, $\Theta = 0$, $n_1^p n_2^q - n_2^p n_1^q = 0$, $n_1^p n_1^q - n_2^p n_2^q = \cos 2\theta$, $X = a(s-t)\sin\theta$ and $Y = a(s+t)\cos\theta + 2d$. Substituting these results into (2.10) and (2.11), gives

$$\frac{\partial^2 G}{\partial n_p \partial n_q} = \mathscr{S}(R) + l^2 \mathscr{H}(X,Y), \tag{3.1}$$

where

$$\begin{aligned} \mathscr{S}(R) &= (l/R)K_1(lR), \\ \mathscr{H}(X,Y) &= \tfrac{1}{2}K_2(lR_1)\cos 2\Theta_1 + K_1(lR_1)\cos\Theta_1\cos\beta \\ &\quad + (2\cos^2\beta - \tfrac{1}{2}\cos 2\theta)K_0(lR_1) + \mathscr{K}_1(\cos 2\theta - \cos 2\beta)\cot\beta, \end{aligned} \tag{3.2}$$

and $\mathscr{K}_1$ is defined by (2.12).

For computations, we simplify (3.1) as follows. Consider the singular term (3.2). Expanding $K_1(lR)$, we find that

$$\mathscr{S}(R) = R^{-2} + \tfrac{1}{2}l^2\log\left(\tfrac{1}{2}lR\right) + l^2\mathscr{R}(R)$$

where

$$\mathscr{R}(R) = (lR)^{-1}K_1(lR) - (lR)^{-2} - \tfrac{1}{2}\log\left(\tfrac{1}{2}lR\right). \tag{3.3}$$

We can see that there is a hypersingular term (R^{-2}), a logarithmically singular term and a regular term ($\mathscr{R}$). For the regular term, we can use the expansion

$$\mathscr{R}(R) = \frac{1}{2}\log\left(\frac{lR}{2}\right)\sum_{m=1}^{\infty}\frac{(lR/2)^{2m}}{m!\,(m+1)!} - \frac{1}{4}\sum_{m=0}^{\infty}\frac{\psi(m+1)+\psi(m+2)}{m!\,(m+1)!}\left(\frac{lR}{2}\right)^{2m}$$

when lR is small, where $\psi(m)$ is the digamma function; for larger lR, we simply use its definition (3.3). Hence, the integral equation (2.9) can be written as

$$\oint_{-1}^{1} \frac{f(t)}{(s-t)^2}\,\mathrm{d}t + (la)^2 \int_{-1}^{1} f(t)\,K(s,t)\,\mathrm{d}t = 0, \qquad -1 < t < 1, \tag{3.4}$$

where $f(t) \equiv [\phi(q(t))]$, $f(\pm 1) = 0$ and

$$K(s,t) = \tfrac{1}{2}\log\left(\tfrac{1}{2}la|s-t|\right) + \mathscr{R}(a|s-t|) + \mathscr{H}(X,Y);$$

both $\mathscr{R}$ and $\mathscr{H}$ are non-singular.

3.2. *Numerical procedure*

To solve the integral equation (3.4), we adopt the procedure used by Parsons & Martin (1992) for scattering problems. Thus, we choose the expansion

$$f(t) \cong (1-t^2)^{1/2} \sum_{n=0}^{N} a_n U_n(t) \tag{3.5}$$

and then collocate at s_j, $j = 0, 1, \ldots, N$, using the collocation points

$$s_j = \cos\left(\frac{(2j+1)\pi}{2N+2}\right), \qquad j = 0, 1, \ldots, N;$$

$U_n(t)$ is a Chebyshev polynomial of the second kind, defined by

$$U_n(\cos\psi) = \frac{\sin(n+1)\psi}{\sin\psi}. \tag{3.6}$$

Our experience with scattering problems and the theoretical results of Golberg (1983, 1985) assure us that the above expansion-collocation method is efficient and effective: the method is uniformly convergent. So, substituting (3.5) into (3.4) and collocating, we find that

$$\sum_{n=0}^{N} a_n B_n(s_j) = 0, \qquad j = 0, 1, \ldots, N, \tag{3.7}$$

where

$$B_n(s_j) = \mathscr{S}_n(s_j) + (la)^2 \int_{-1}^{1} (1-t^2)^{1/2} U_n(t) \mathscr{H}(X,Y)\,\mathrm{d}t,$$

$$\mathscr{S}_n(s) = \oint_{-1}^{1} \frac{(1-t^2)^{1/2} U_n(t)}{(s-t)^2}\,\mathrm{d}t + (la)^2 \int_{-1}^{1} (1-t^2)^{1/2}\, U_n(t)\, \mathscr{R}(a|s-t|)\,\mathrm{d}t + (la)^2 \mathscr{W}_n(s), \tag{3.8}$$

$$\mathscr{W}_n(s) = \frac{1}{2}\int_{-1}^{1} (1-t^2)^{1/2}\, U_n(t)\, \log\left(\tfrac{1}{2}la|s-t|\right)\,\mathrm{d}t \tag{3.9}$$

and X, Y are evaluated at $s = s_j$. Before we discuss the procedure for finding non-trivial solutions to (3.7), we note three results of use in evaluating (3.8) and (3.9). First, we have the well-known relation

$$\oint_{-1}^{1} \frac{(1-t^2)^{1/2}\, U_n(t)}{(s-t)^2}\,\mathrm{d}t = -\pi(n+1)U_n(s).$$

This result is one of the main advantages of the above scheme, whereby any difficulty encountered in evaluating Hadamard finite-part integrals numerically is conveniently

avoided. The integral $\mathscr{W}_n$ is evaluated in Appendix B:

$$\mathscr{W}_0 = \frac{\pi}{4}\left\{\frac{T_2(s)}{2} + \log\frac{la}{4}\right\}, \qquad \mathscr{W}_n = \frac{\pi}{4}\left\{\frac{T_{n+2}(s)}{n+2} - \frac{T_n(s)}{n}\right\} \tag{3.10}$$

for $n \geqslant 1$, where T_n is a Chebyshev polynomial of the first kind. Finally, we note that the collocation points which we use are symmetric around $s = 0$. With this knowledge, we can make use of two properties of $\mathscr{S}_n$, namely, $\mathscr{S}_n(s) = \mathscr{S}_n(-s)$ when n is even and $\mathscr{S}_n(s) = -\mathscr{S}_n(-s)$ when n is odd (these are easily derived by letting $s = -s$ and $t = -t$ in the definition of $\mathscr{S}_n$, and then using the even/odd properties of U_n). Moreover, for *horizontal* plates, we can go further, for then we have $B_n(s) = B_n(-s)$ when n is even and $B_n(s) = -B_n(-s)$ when n is odd. These last two properties are useful in reducing computation time for what turns out to be a lengthy process.

To find non-trivial solutions of the problem, we see from (3.7) that we need to search for parameters d, θ, l and β, such that the determinant of $B_n(s_j)$ vanishes. Clearly, a random choice of these parameters is highly unlikely to meet this criterion. However, it is possible to derive an approximate formula for finding trapped modes above a *horizontal* plate ($\theta = 0$). This special geometry is discussed next.

3.3. *Horizontal flat plates*

Linton & Evans (1991) obtained an approximate formula for the trapped-mode frequencies for a horizontal plate in water of constant finite depth, h; the plate has length $2a$ and is submerged at depth d beneath the free surface. It is assumed that the plate is long, so that the two edges of the plate only interact via waves that propagate back and forth between them above the plate; this is a typical *wide-spacing approximation*. The main ingredient in the approximation is the reflection coefficient for such a wave above a *semi-infinite* plate, and this can be found by solving the corresponding boundary-value problem using the Wiener–Hopf technique.

We have obtained the analogous formula for deep water in two ways. First, we have solved the deep-water boundary-value problem (Parsons 1994) using the Wiener–Hopf technique, as used for a similar problem by Greene & Heins (1953). This leads to the formula

$$F(l) = \alpha a + m\pi, \tag{3.11}$$

where

$$F(l) = F_0 + \frac{3\pi}{4} + \frac{1}{2}\tan^{-1}\frac{\psi}{K} + \frac{\alpha}{\pi K} + \frac{k}{\pi K}\log\frac{k-\alpha}{l} - \frac{1}{\pi K}\int_0^{\alpha}\frac{t(t^2+l^2)^{1/2}}{t^2+\psi^2}\log\left(\frac{(t^2+l^2)^{1/2}-t}{l}\right)\mathrm{d}t, \tag{3.12}$$

$$F_0 = \frac{\alpha d}{\pi}\left\{\log\frac{ld}{2\pi} + \gamma - 1\right\} - \frac{kd}{\pi}\log\frac{k-\alpha}{l} - \tan^{-1}\frac{\alpha}{\psi} - \frac{1}{2}\tan^{-1}\frac{l}{\alpha} - \frac{1}{\pi}\tan^{-1}\frac{\psi}{K}\tan^{-1}\frac{\psi}{\alpha} + \sum_{n=1}^{\infty}\left\{\tan^{-1}\left(\frac{\alpha}{(l^2+\kappa_n^2)^{1/2}}\right) - \frac{\alpha d}{n\pi}\right\}, \tag{3.13}$$

$\alpha = (k^2 - l^2)^{1/2}$, $\psi = (l^2 - K^2)^{1/2}$, k is the positive real root of $K = kd\tanh kd$, κ_n are the positive real roots of

$$K + \kappa_n \tan\kappa_n d = 0, \qquad n = 1, 2, \ldots,$$

satisfying $(n - \frac{1}{2})\pi < \kappa_n d < n\pi$, and $\gamma = 0.5772\ldots$ is Euler's constant. (We shall

discuss the use of (3.11) shortly.) Note that the integral in (3.12) cannot be evaluated in closed form, although it can be evaluated numerically without difficulty.

Second, we have taken the formula obtained by Linton & Evans (1991) for finite h and then calculated the limit as $h \to \infty$ (Martin 1994). The result is (3.11) with

$$F(l) = F_0 + \frac{1}{2\pi} \log \frac{k-\alpha}{l} \log \frac{k+K}{k-K} - \frac{1}{\pi} \mathrm{Li}_2(\mathrm{e}^{-A}, \delta) + \frac{1}{\pi} \mathrm{Li}_2(\mathrm{e}^{-A}, \pi + \delta),$$

where $A = \sinh^{-1}(\alpha/l) = -\log((k-\alpha)/l)$, $\delta = \tan^{-1}(\psi/K)$ and F_0 is defined by (3.13). Here, the dilogarithm is defined by (Lewin 1958)

$$\mathrm{Li}_2(z) = -\int_0^z \log(1-w) \frac{\mathrm{d}w}{w}$$

for complex z, and

$$\mathrm{Li}_2(r, \theta) = \mathrm{Re}\left\{\mathrm{Li}_2(r\mathrm{e}^{\mathrm{i}\theta})\right\} = -\tfrac{1}{2} \int_0^r \log(1 - 2x\cos\theta + x^2) \frac{\mathrm{d}x}{x}.$$

We have also shown that the two formulae for $F(l)$ are equivalent (Parsons 1994).

In (3.11), $2a$ is the plate length and m is any integer. Equation (3.11) gives approximations to symmetric modes; for antisymmetric modes, $\pi/2$ must be subtracted from the definition of $F(l)$. The way we use this formula is to fix K, d and a, thus fixing k. For trapped modes, the wavenumber l is then known to lie in the interval $K < l < k$ (Linton & Evans 1991). Equation (3.11) is then used by varying l from $l = K$ to $l = k$ until all solutions have been found. Varying m will give rise to different modes (if they exist); in practice, it was found that solutions of (3.11) only exist when $m \leqslant 0$ for both symmetric and antisymmetric modes. We use the bisection method to trap l until l is correct to four decimal places (as far as the approximation is concerned, that is). This wide-spacing approximation can then be used as a starting point for the numerical solution and the true solution sought. The determinant of $B_n(s_j)$ will change sign as we pass through the true solution, and so, again, we can use the bisection method to converge on l.

The way in which the trapped-mode frequencies were calculated was first to use the wide-spacing formula as just discussed, and then to carefully check the results with the numerical solution obtained from the hypersingular integral-equation formulation. In practice, it proved convenient to scale the matrix $B_n(s_j)$, $j, n = 0, 1, \ldots, N$, by dividing through by its largest element. This bounds the determinant by unity without affecting the position of any zeros thereof; in all cases, the largest element was found to be $B_N(s_N)$. It was found that the wide-spacing approximation was accurate to three decimal places virtually throughout, thus speeding up dramatically the final numerical process. One other advantage of the wide-spacing approximation is that symmetric and antisymmetric modes are distinguished, whereas this is not so for the numerical solution (although this could be incorporated for symmetric geometries).

3.4. *Results for inclined plates*

We now discuss the results obtained for an inclined plate. Of course, the wide-spacing approximation is no longer valid for this geometry, and so we resort to a full numerical solution. However, the horizontal-plate result is still important in giving a starting point from which to follow the trapped-mode frequencies as the plate is rotated through to the vertical. The solution was followed manually as the plate was moved from the horizontal, until a pattern could be seen from which to automate the process. In tracking the zeros of the determinant, it is important

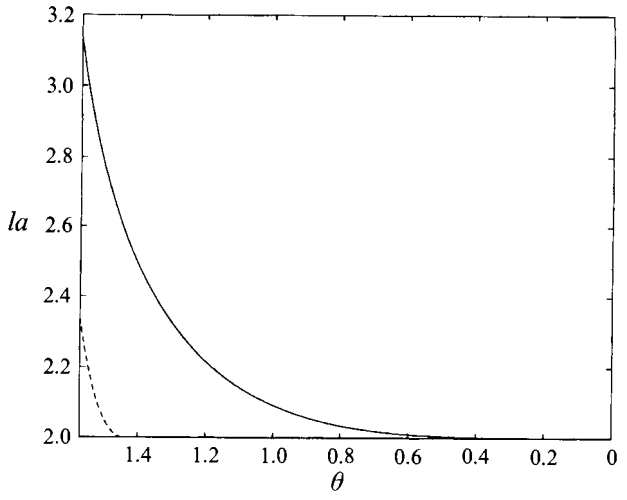

FIGURE 2. Graphs of la against θ, where θ is the angle between the plate and the vertical, for the trapped modes above a submerged, flat plate when $a/c = 5$, $Ka = 2$ and c is the distance from the upper plate edge to the free surface: — represents a mode which is symmetric when the plate is horizontal; similarly — — represents a mode which is antisymmetric for the horizontal plate.

(in view of the lengthy computation required) to estimate the interval in which the root lies as accurately as possible, thereby reducing the number of bisections required to achieve a desired accuracy. So, for decreasing θ we chose to start by using the previous solution for l as the new upper bound for the search, and to estimate a lower bound from the manual computation carried out. However, the computation was checked at regular intervals to enable a more refined interval for the new root to be found. Figure 2 contains graphs of la against θ for $a/c = 5$ and $Ka = 2$. Here, c is the distance from the upper plate edge to the free surface (whence $d = c + a\cos\theta$). For this geometry, we have one symmetric mode and also one antisymmetric mode for the horizontal plate. However, rotating the plate will break the symmetry. We can see that the value of l gets smaller as soon as the plate is rotated. It also appears that the smaller the value of l with which we start, the quicker it reduces. The mode which started as antisymmetric quickly reaches the lower cut-off at $l = 2$ and disappears when $\theta \approx 83°$ (horizontal is 90°). The other mode continues until the plate is vertical, when it eventually disappears.

Figure 3 contains a similar graph, this time with $a/c = 10$ and $Ka = 4$. The flat plate starts off with two symmetric modes and two antisymmetric modes. Again, we see a decrease in l as θ is decreased. The smallest mode disappears almost immediately, at about $\theta = 89.5°$. The next two modes reach the lower cut-off at about $\theta = 85°$ and $\theta = 75°$. Again, we see the mode which started off as the largest symmetric mode continuing right up until the plate is vertical. We note that the modes never cross over each other for any value of θ. The results presented here were found using $N = 20$ and an accuracy of three decimal places was required.

4. Curved plates

We now extend the previous work and look at the possibility of trapped modes existing above a submerged, thin, curved plate, on deep water. In principle, the

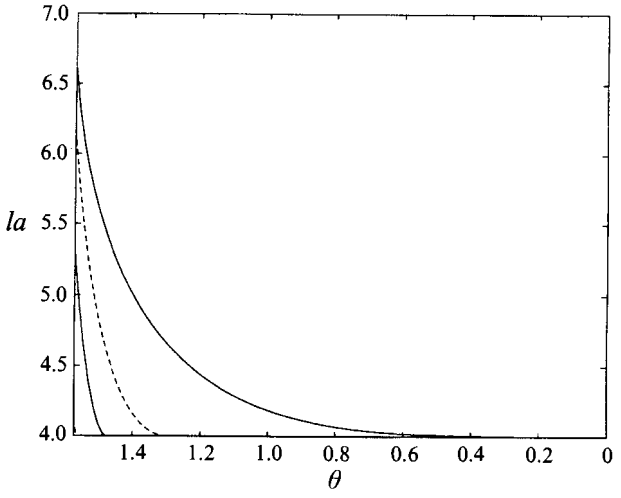

FIGURE 3. Graphs of la against θ, where θ is the angle between the plate and the vertical, for the trapped modes above a submerged, flat plate when $a/c = 10$, $Ka = 4$ and c is the distance from the upper plate edge to the free surface: — represents modes which are symmetric when the plate is horizontal; similarly —— represents modes which are antisymmetric for the horizontal plate.

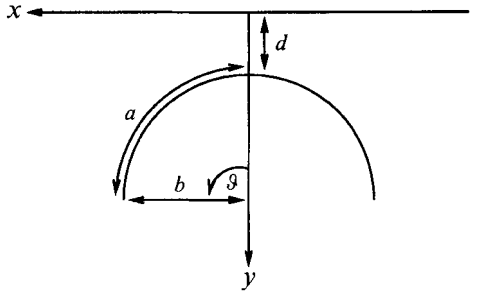

FIGURE 4. Geometry of the submerged, curved plate.

integral-equation method is applicable to smooth curves Γ of any shape. However, we shall limit ourselves to circular arcs with a vertical line of symmetry; see figure 4. The circle is centred at $(0, b+d)$ and has radius b; the arc has length $2a = 2b\vartheta$. The virtue of this choice for Γ is that we can check the results in two ways. First, for suitably chosen parameters, we have an almost flat plate, whereby the results from §3 can be used for comparison and also as a starting point from which to follow the trapped modes as the curvature of the plate is increased. Secondly, McIver & Evans (1985) considered the trapping of surface waves above a submerged, horizontal, circular cylinder, on deep water, using a numerical procedure based on the analysis of Ursell (1951). We expect to recover their results as the circular arc approaches a complete circle.

So, we wish to solve the homogeneous, hypersingular integral equation (2.9), subject to $[\phi] = 0$ at the two edges of Γ. We parametrize the circular arc using

$$\xi(t) = b\sin(t\vartheta), \qquad \eta(t) = d + b - b\cos(t\vartheta), \qquad -1 \leqslant t \leqslant 1.$$

It follows that

$$X = b(\sin(s\vartheta) - \sin(t\vartheta)), \qquad Y = 2d + 2b - b(\cos(s\vartheta) + \cos(t\vartheta)),$$

$$\boldsymbol{n}(p) = (-\sin(s\vartheta), \cos(s\vartheta)), \qquad \boldsymbol{n}(q) = (-\sin(t\vartheta), \cos(t\vartheta)), \qquad \mathscr{N} = \cos(s-t)\vartheta,$$

$$n_1^p n_2^q - n_2^p n_1^q = -\sin(s-t)\vartheta, \qquad n_1^p n_1^q - n_2^p n_2^q = -\cos(s+t)\vartheta,$$

$$R = 2b\sin(|s-t|\vartheta/2) \tag{4.1}$$

and $\Theta = -\frac{1}{4}R^4/b^2$. From (2.10), the kernel of (2.9) is given by (3.1), where $\mathscr{H}(X, Y)$ can easily be evaluated from its definition, (2.11), and

$$\begin{aligned}\mathscr{S}(R) &= b^{-2}\{(b^2 - \tfrac{1}{2}R^2)(l/R)K_1(lR) + \tfrac{1}{4}(lR)^2 K_2(lR)\} \\ &= R^{-2} + \tfrac{1}{2}l^2\log(\tfrac{1}{2}lR) + l^2\mathscr{R}(R);\end{aligned}$$

the second equality defines the non-singular function $\mathscr{R}$. Now, from (4.1), we have

$$R^{-2} = (a|s-t|)^{-2} + a^{-2}\mathscr{R}_1(|s-t|),$$
$$\log(\tfrac{1}{2}lR) = \log(\tfrac{1}{2}la|s-t|) + \mathscr{R}_2(|s-t|)$$

where

$$\mathscr{R}_1(w) = (\tfrac{1}{2}\vartheta)^2\{\sin(\tfrac{1}{2}w\vartheta)\}^{-2} - w^{-2} \quad \text{and} \quad \mathscr{R}_2(w) = \log\left(\frac{\sin(w\vartheta/2)}{w\vartheta/2}\right).$$

Hence, parametrizing (2.9) gives a one-dimensional, homogeneous, hypersingular integral equation, which we write as

$$\text{⨍}\!\!\!\!\!\!-\!\!\int_{-1}^{1} \frac{f(t)}{(s-t)^2}\,\mathrm{d}t + \int_{-1}^{1} f(t)\,\mathscr{R}_1(|s-t|)\,\mathrm{d}t + (la)^2\int_{-1}^{1} f(t)\,K(s,t)\,\mathrm{d}t = 0, \qquad -1 < t < 1,$$

where

$$K(s,t) = \tfrac{1}{2}\log(\tfrac{1}{2}la|s-t|) + \tfrac{1}{2}\mathscr{R}_2(|s-t|) + \mathscr{R}(R) + \mathscr{H}(X,Y).$$

Thus, we have isolated the hypersingular term and the logarithmically singular term. All the remaining kernels, $\mathscr{R}$, $\mathscr{R}_1$, $\mathscr{R}_2$ and $\mathscr{H}$, are non-singular and easily computed, either from their definitions or from expansions in $|s-t|$ as appropriate (Parsons 1994).

4.1. *Numerical procedure*

The numerical procedure now follows that of §3.2. We substitute the expansion (3.5) for $f(t)$ and collocate at s_j, $j = 0, 1, \ldots, N$, giving the homogeneous equation

$$\sum_{n=0}^{N} a_n D_n(s_j) = 0, \qquad j = 0, 1, \ldots, N,$$

where

$$D_n(s_j) = \text{⨍}\!\!\!\!\!\!-\!\!\int_{-1}^{1} \frac{(1-t^2)^{1/2}U_n(t)}{(s_j-t)^2}\,\mathrm{d}t + \int_{-1}^{1}(1-t^2)^{1/2}\,U_n(t)\,\mathscr{R}_1(|s_j-t|)\,\mathrm{d}t$$
$$+ (la)^2\int_{-1}^{1}(1-t^2)^{1/2}U_n(t)\,K(s_j,t)\,\mathrm{d}t.$$

The hypersingular integral and the logarithmically singular integral can both be evaluated exactly as in §3.2. It can be shown that $D_n(s)$ has the following properties: $D_n(s) = D_n(-s)$ when n is even and $D_n(s) = -D_n(-s)$ when n is odd, thereby halving

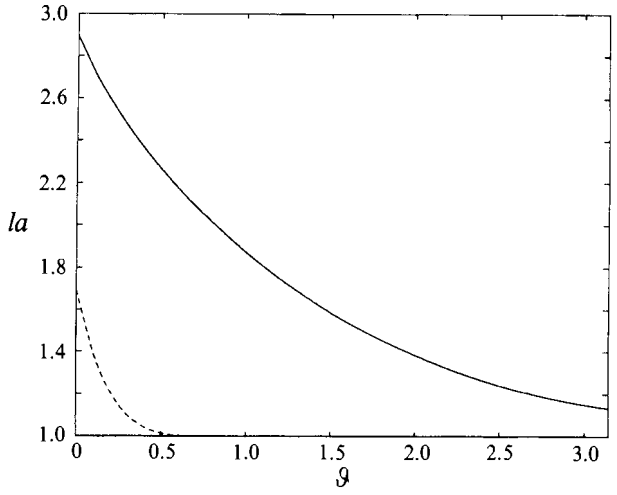

FIGURE 5. Graphs of la against ϑ for the trapped modes above a submerged, curved plate when $a/d = 10$ and $Ka = 1$: — represents a mode which is symmetric in the limit $\vartheta \to 0$ (that is, a flat plate); and —— represents an antisymmetric mode in this same limit.

computation time in all cases. Again, a non-trivial solution is given by the vanishing of the determinant of $D_n(s_j)$.

4.2. *Results*

For the curved plate, we sometimes choose to non-dimensionalize with respect to the length of the plate, $2a = 2b\vartheta$, and sometimes with respect to the radius, b, as convenient.

Figure 5 shows graphs of la against ϑ for $Ka = 1$ and $a/d = 10$ (in effect, *bending* the plate towards a circular cylinder). We start off from the horizontal plate solution, where a symmetric and an antisymmetric mode are found, and follow them as ϑ is increased. We can see that the smaller mode vanishes when $\vartheta \approx 30°$. However, the other solution does not vanish, and can be seen to remain as we approach $\vartheta = \pi$. Clearly, we cannot reach π using this method of solution, as we have assumed that $[\phi] = 0$ at both edges of the plate. However, we can get close enough so that the result can be used to help find another type of solution: we non-dimensionalize with respect to πb, and then reduce ϑ. The reason for this choice is that in the limit $\vartheta \to \pi$, we have $a = b\pi$ and so we are fixing the radius of the plate to match up with the solution that we have just found. Reducing ϑ now corresponds to reducing the length of the plate, thereby giving a different solution.

Figure 6 shows the graph of $l\pi b$ against ϑ for $K\pi b = 1$ and $\pi b/d = 10$. At first, the graph changes slowly as we reduce ϑ. However, after $\vartheta \approx 130°$ the solution quickly decreases towards the lower cut-off, and, of course, as the plate vanishes when $\vartheta = 0$, so does the solution. However, numerically at least, the solution does appear to remain for all $\vartheta > 0$.

We continue with this approach in figures 7 and 8. This time all the parameters remain the same except K, so that in figure 7 we plot la against ϑ for $Ka = 4$ and $a/d = 10$. Again, starting off from the flat-plate solution, we have two symmetric and two antisymmetric modes to follow. As can be seen from figure 7, the smallest of these modes vanishes almost immediately. The next two vanish at about $\vartheta \approx 30°$ and 115°. Again, however, we see that the largest solution remains all the way up

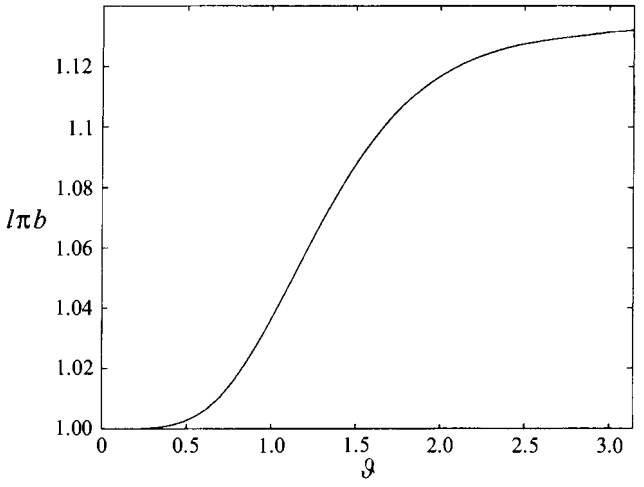

FIGURE 6. Graph of $l\pi b$ against ϑ for the trapped mode above a submerged, curved plate when $K\pi b = 1$ and $\pi b/d = 10$.

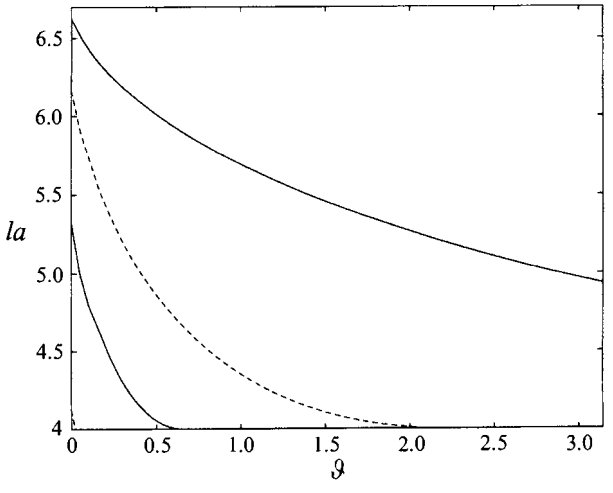

FIGURE 7. Graphs of la against ϑ for the trapped modes above a submerged, curved plate when $a/d = 10$ and $Ka = 4$: — represents modes which are symmetric in the limit $\vartheta \to 0$ (that is, a flat plate); and —— represents antisymmetric modes in this same limit.

until we approach π, and is still above the lower cut-off. Reversing the process, as before, by non-dimensionalizing with respect to πb, we can see that the solution hardly changes as we reduce ϑ until we reach $\vartheta \approx 70°$. After that, the solution changes dramatically, rapidly approaching the lower cut-off, before vanishing along with the plate. We can explain these results as follows. By keeping the plate length fixed and varying ϑ, the effect of deforming the plate will be felt along its entire length, including the point closest to the free surface. However, by fixing the radius b and then varying ϑ, the main difference will be caused by the fluid motion at the two edges of the plate. Therefore, as we increase K, the significant fluid motion becomes restricted to a thin layer near the free surface, and is little affected by the plate edges.

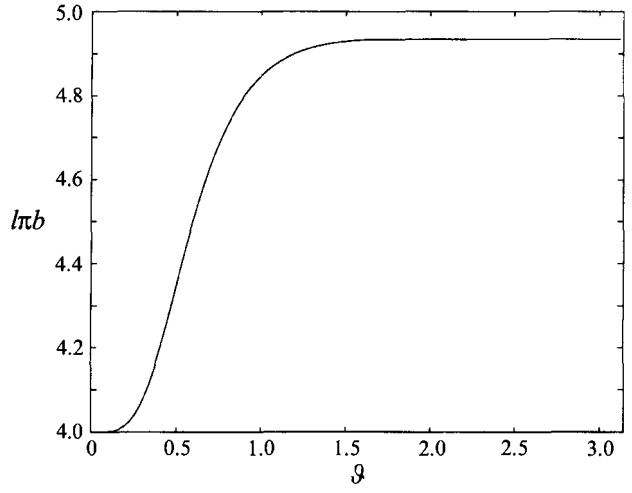

FIGURE 8. Graph of $l\pi b$ against ϑ for the trapped mode above a submerged, curved plate when $K\pi b = 4$ and $\pi b/d = 10$.

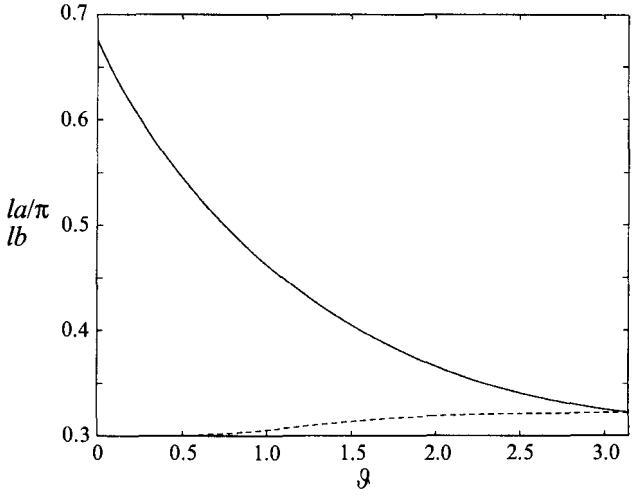

FIGURE 9. Graph of la/π against ϑ for the trapped mode above a submerged, curved plate when $Ka/\pi = 0.3$ and $a/d\pi = 2$ (—). Also shown is the graph of lb against ϑ for the trapped mode above a submerged, curved plate when $Kb = 0.3$ and $b/d = 2$ (– –).

Although we know that the method is converging to the correct solutions as the plate approaches the flat-plate solution, it is desirable to check its validity at the other extreme. In fact, it is possible to compare with the solutions of McIver & Evans (1985) for a submerged, horizontal circular cylinder, given a suitable choice of parameters. This has been done extensively, and in all cases the results were found to be in agreement. As an example, figure 9 contains two graphs whose starting value was taken from the above paper.

First, we follow their solution for a symmetric, trapped mode above a submerged circular cylinder, for $Kb = 0.3$ and $b/d = 2$, by non-dimensionalizing with respect to the radius b. This is straightforward: we merely set Kb and b/d as above and then

vary ϑ; the results are given by the broken curve. Secondly, we non-dimensionalize with respect to the length of the plate. To this end, it proves convenient to non-dimensionalize by a/π, so that the solution matches the other one for $\vartheta = \pi$; the results are given by the solid curve. We see similar behaviour as before, with the fixed-radius solution vanishing along with the plate, and the fixed-length solution continuing up to the flat-plate solution. For the flat-plate limit, we can use either the approximate solution or the full numerical solution, or both, as shown in §3. We find that the mode is symmetric in this limit and is seen to be the only one in existence for the given geometry. It is clear that a mode which starts off symmetric and ends up symmetric, above a symmetric geometry, must itself be symmetric.

N.F.P. was supported by a studentship from the SERC.

Appendix A. Computation of $L_m(x)$

For the evaluation of $L_m(x)$, defined by (2.7), we have several options. For example, Abramowitz & Stegun (1965) gives several series expansions. However, for large x and for many values of m, this is an inefficient method. Another possibility is to use an integral representation given Apelblat & Kravitsky (1985), but this is also inefficient when many values of m and x are required. We therefore turn our attention to the use of recurrence relations. These can be derived by differentiating the (homogeneous) recurrence relations for the modified Bessel function $I_\nu(x)$ with respect to ν, and then setting $\nu = m$. Thus, we obtain the following inhomogeneous recurrence relations for L_m:

$$\begin{aligned} L_{m-1}(x) - L_{m+1}(x) - (2m/x)L_m(x) &= (2/x)I_m(x), \\ L'_m(x) - L_{m+1}(x) - (m/x)L_m(x) &= (1/x)I_m(x). \end{aligned} \tag{A 1}$$

Consider (A 1). At first sight, it appears that we can use this in the forward direction with starting values $L_0(x) = -K_0(x)$ and $L_1(x) = K_1(x) - I_0(x)/x$. However, owing to severe accumulation of rounding errors, this approach turns out to be misguided, as is the case when forward recurrence is used for the computation of I_n or J_n. Instead, we use what is known as the *Wimp–Luke* method (Wimp 1984). Fix M as an integer somewhat larger than the largest value of m required. Then, generate a solution Z_m of the inhomogeneous equation, (A 1), in the *backwards* direction, with the starting values

$$Z_{M+1} = Z_M = 0.$$

Next, generate a solution Y_m of the homogeneous equation (with the right-hand side of (A 1) replaced by zero), again in the backwards direction but with the starting values

$$Y_{M+1} = 0 \quad \text{and} \quad Y_M = 1.$$

The desired solution of (A 1) is then formed by letting

$$L_m \simeq \left(\frac{L_0 - Z_0}{Y_0}\right) Y_m + Z_m, \qquad 0 \leqslant m \leqslant M+1, \tag{A 2}$$

where $L_0 = -K_0(x)$. In fact, the general solution (A 2) is slightly simplified for our problem, since $Y_m/Y_0 \equiv I_m/I_0$, whence

$$L_m \simeq -\left(\frac{K_0 + Z_0}{I_0}\right) I_m + Z_m, \qquad 0 \leqslant m \leqslant M+1.$$

To achieve greater accuracy, we can iterate: take L_M and L_{M-1} as new starting values for Z_M and Z_{M-1}, respectively, and then repeat the above procedure. This process can be repeated. In practice, provided M is chosen slightly greater than the maximum value of m required in the summation containing L_m, and only one iteration is performed, the results are found to be excellent.

Appendix B. Evaluation of $\mathscr{W}_n$

$\mathscr{W}_n$ is defined by (3.9). Using (3.6), we obtain

$$\mathscr{W}_n = \tfrac{1}{4}(\mathscr{V}_n - \mathscr{V}_{n+2}), \tag{B 1}$$

where

$$\mathscr{V}_n = \int_0^\pi \cos n\psi \, \log\left(\tfrac{1}{2}la|s - \cos\psi|\right) \, \mathrm{d}\psi.$$

Using the expansion

$$\log|s-t| = -\log 2 - 2\sum_{m=1}^{\infty} \frac{1}{m} T_m(s)\, T_m(t),$$

and $T_m(\cos\psi) = \cos m\psi$, we can easily integrate over ψ to give

$$\mathscr{V}_0 = \pi \log(la/4) \quad \text{and} \quad \mathscr{V}_n = -(\pi/n)T_n(s)$$

for $n \geqslant 1$. The result (3.10) follows from (B 1).

REFERENCES

Abramowitz, M. & Stegun, I. A. (eds.) 1965 *Handbook of Mathematical Functions*. Dover.

Apelblat, A. & Kravitsky, N. 1985 Integral representations of derivatives and integrals with respect to order of the Bessel functions $J_\nu(t)$, $I_\nu(t)$ the Anger function $\mathbf{J}_\nu(t)$ and the integral Bessel function $Ji_\nu(t)$. *IMA J. Appl. Maths* **34**, 187–210.

Bonnet-Ben Dhia, A.-S. & Joly, P. 1993 Mathematical analysis of guided water waves. *SIAM J. Appl. Maths* **53**, 1507–1550.

Golberg, M. A. 1983 The convergence of several algorithms for solving integral equations with finite-part integrals. *J. Integ. Equat.* **5**, 329–340.

Golberg, M. A. 1985 The convergence of several algorithms for solving integral equations with finite-part integrals. II. *J. Integ. Equat.* **9**, 267–275.

Greene, T. R. & Heins, A. E. 1953 Water waves over a channel of infinite depth. *Q. Appl. Maths* **11**, 201–214.

Jones, D. S. 1953 The eigenvalues of $\nabla^2 u + \lambda u = 0$ when the boundary conditions are given in semi-infinite domains. *Proc. Camb. Phil. Soc.* **49**, 668–684.

LeBlond, P. H. & Mysak, L. A. 1978 *Waves in the Ocean*. Elsevier.

Lewin, L. 1958 *Dilogarithms and Associated Functions*. Macdonald.

Linton, C. M. & Evans, D. V. 1991 Trapped modes above a submerged horizontal plate. *Q. J. Mech. Appl. Maths* **44**, 487–506.

McIver, P. & Evans, D. V. 1985 The trapping of surface waves above a submerged, horizontal cylinder. *J. Fluid Mech.* **151**, 243–255.

Martin, P. A. 1989 On the computation and excitation of trapping modes. *Proc. 4th Intl Workshop on Water Waves and Floating Bodies*, Øystese, Norway (ed. J. Grue), pp. 145–147. University of Oslo.

Martin, P. A. 1994 Asymptotic approximations for functions defined by series, with some applications to the theory of guided waves. Preprint.

Martin, P. A. & Rizzo, F. J. 1989 On boundary integral equations for crack problems. *Proc. R. Soc. Lond.* A **421**, 341–355.

MEYER, R. E. 1971 Resonance of unbounded water bodies. In *Mathematical Problems in Geophysical Sciences*, vol. 1 (ed. W. H. Reid), pp. 189–227. American Mathematical Society, Providence.

PARSONS, N. F. 1994 The interaction of water waves with thin plates. PhD thesis. University of Manchester, UK.

PARSONS, N. F. & MARTIN, P. A. 1992 Scattering of water waves by submerged plates using hypersingular integral equations. *Appl. Ocean Res.* **14**, 313–321.

PARSONS, N. F. & MARTIN, P. A. 1994 Scattering of water waves by submerged curved plates and by surface-piercing flat plates. *Appl. Ocean Res.* **16**, 129–139.

URSELL, F. 1951 Trapping modes in the theory of surface waves. *Proc. Camb. Phil. Soc.* **47**, 347–358.

URSELL, F. 1952 Edge waves on a sloping beach. *Proc. R. Soc. Lond.* A **214**, 79–97.

URSELL, F. 1962 Slender oscillating ships at zero forward speed. *J. Fluid Mech.* **14**, 496–516.

URSELL, F. 1968 The expansion of water-wave potentials at great distances. *Proc. Camb. Phil. Soc.* **64**, 811–826.

WIMP, J. 1984 *Computation with Recurrence Relations.* Pitman.